

SEARCHES FOR $K_L^0 \rightarrow \pi^0 \nu \bar{\nu}$

JIASEN MA* and YAU W. WAH†

*The Enrico Fermi Institute, The University of Chicago,
 Chicago, Illinois 60637, USA*

*jsma@uchicago.edu

†ywah@uchicago.edu

Received 4 August 2012

Published 6 December 2012

The physics potential of the $K_L^0 \rightarrow \pi^0 \nu \bar{\nu}$ search is summarized. Past experiments and the challenges discovered in them are reviewed. The innovative methods employed by the current experiment are discussed. Future experimental prospects are given.

Keywords: Direct CP violation; CKM matrix; K meson rare decays; KOTO.

PACS Number(s): 13.20.Eb, 12.15.Hh, 14.40.Df

1. Introduction

The CKM matrix¹ in the Standard Model has been very successful in describing the known Charge Conjugation Parity symmetry (CP) violations.^{2–7} However the CP violation magnitude implied by the Standard Model is too small to explain the matter-dominant universe.⁸ Searching for new CP violation is of great relevance.

$K_L^0 \rightarrow \pi^0 \nu \bar{\nu}$, which is yet to be observed, is a unique test ground for the CP violation. The decay is a direct CP violating process. Its branching ratio measures the CP violation parameter in the Standard Model.⁹ The branching ratio is highly suppressed to $(2.43 \pm 0.39 \pm 0.06) \times 10^{-11}$ in the Standard Model.¹⁰ The bigger uncertainty component here comes from the uncertainty on the Standard Model parameters, while the theoretical uncertainty is about 2% only. Any deviation of a measurement from the prediction will be a clear signal for new physics. Theoretical interest in $K_L^0 \rightarrow \pi^0 \nu \bar{\nu}$ dates back to the 70s.^{11–14} This article mostly focuses on the experimental searches.

2. Past Experiments

To search for such a rare process as $K_L^0 \rightarrow \pi^0 \nu \bar{\nu}$, fixed target approach is preferred to take advantage of the Avogadro's number to produce enough K_L^0 's, which are typically produced by high energy protons hitting heavy metal targets.

Since there are two neutrinos in the $K_L^0 \rightarrow \pi^0 \nu \bar{\nu}$ final state, the classic method of searching for invariant mass peak cannot be applied. The neutral pion bears almost all the burden of the kinematics signature.

The first search for the $K_L^0 \rightarrow \pi^0 \nu \bar{\nu}$ decay mode was done with data collected by E731 at Fermilab in the early 90s. The branching ratio of $K_L^0 \rightarrow \pi^0 \nu \bar{\nu}$ was limited to be $< 2.2 \times 10^{-4}$ (90% CL).¹⁵ In this search, the π^0 Dalitz decay ($\pi^0 \rightarrow e^+ e^- \gamma$) provided both the decay vertex and kinematics of the π^0 as the momenta of the electron and positron were measured with tracking devices. This technique was followed by E799-I and E799-II.^{16,17} With around 220 billion K_L^0 decays, the limit was set at $< 5.9 \times 10^{-7}$ (90% CL).¹⁷ The penalty to pay here was the small branching ratio of the π^0 Dalitz decay (1.2%).

If measured via the dominant decay $\pi^0 \rightarrow \gamma \gamma$, the longitudinal vertex position can be measured if one *assumes the two γ 's are from the π^0* . The first search via the 2γ 's mode was performed with the KTeV at Fermilab in the late 90s.¹⁸ The limit set was $< 1.6 \times 10^{-6}$ (90% CL). While the Dalitz decay method can afford to have two neutral beams in E731 and E799, the two γ 's approach needs a single narrow pencil beam to constrain the vertex in the plane perpendicular to the beam to measure the transverse momentum of the π^0 . To make this measurement, one of the two KTeV neutral beams was blocked.

KTeV was optimized for other purposes. The calorimeter measuring photon energies was located outside the vacuum decay region. And there were drift chambers and other material in front of the calorimeter in addition to the vacuum window and air. Neutron interactions with these extra materials were detrimental to the $K_L^0 \rightarrow \pi^0 \nu \bar{\nu}$ search. The result also suffered from the veto non-hermeticity of the detectors. Processes with more two photons could fake the signal. Consequently the KTeV limit was worse than the E799-II result using the small branching ratio π^0 Dalitz decay.

E391a at KEK was the first dedicated experiment for the $K_L^0 \rightarrow \pi^0 \nu \bar{\nu}$ search.¹⁹ It incorporated both the pencil beam and the veto hermeticity. It detected the two γ 's from the π^0 decay in the final state to reconstruct the π^0 . The calorimeter composed of an array of CsI crystals was used to measure the energies of the forwardly boosted photons. A beam hole was left in the center of the array to have the beam pass through. A charged veto detector made of plastic scintillators wrapped around the calorimeter to distinguish charged particle hits in the calorimeter from photon hits. A barrel veto detector formed the K_L^0 decay region with the calorimeter at its downstream end. Smaller veto detectors were installed at the upstream end of the barrel and behind the CsI to ensure a 4π coverage. The entire detector was in vacuum with the exception of some veto detectors downstream from the calorimeter.

With two months of data taking, an upper limit of 2.6×10^{-8} (90% CL) was established with about 9 billion K_L^0 decays.¹⁹ There was no event observed in the signal region. But further running E391a was background limited. The expected

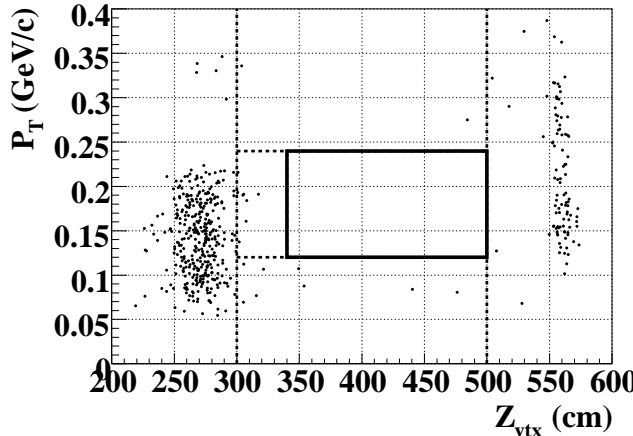


Fig. 1. E391a final result. Reconstructed π^0 transverse momentum vs. vertex. The empty box was the signal region. And the calorimeter front surface was at $Z = 615$ cm. The two bands of events outside the signal box were at the locations where two detectors (CC02 and CV) surrounding the beam were located.

background was (0.9 ± 0.4) for a single event sensitivity of $(1.1 \pm 0.1) \times 10^{-8}$.¹⁹ The background mainly came from the halo neutron interaction with detectors close to the beam and the decay region. The halo neutrons hitting the detectors surrounding the beam were not suppressed enough. The final result of E391a is shown in Fig. 1 to illustrate the background from halo neutron interactions.

3. The KOTO Experiment

The KOTO experiment is a neutral Kaon rare decay experiment at J-PARC. The primary goal is to make the first observation of the Standard Model $K_L^0 \rightarrow \pi^0 \nu \bar{\nu}$ events. It is in preparation as of August 2012. From 2010 to 2012, a series of engineering runs were conducted to test the performance of the beamline and the detectors. Physics run is expected to start in early 2013.

The KOTO experiment aims for a 3 orders of magnitude improvement²⁰ in sensitivity over the previous generation of experiment-E391a. A major upgrade is necessary not only in the number of K_L^0 decay collected, but also in background suppression. A cross-section view of the detector system is shown in Fig. 2. The basic layout is very similar as the E391a experiment with the same basics strategy. However with the exception of the mechanical structure such as the vacuum tank, all KOTO detectors and the beamline are newly made or reinforced.

In the following sections, the upgrades enabling the over 1000 times improvement are discussed.

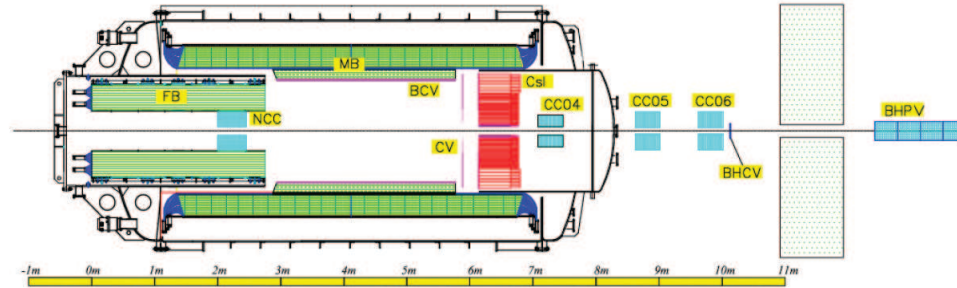


Fig. 2. Detector cross-section view. The neutral beam with K_L^0 's comes from the left.

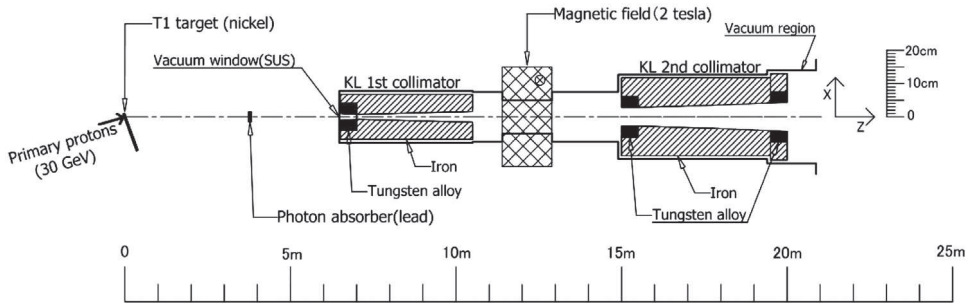


Fig. 3. Schematic drawing of the beamline. It was fabricated and installed in 2009. Both ends of the two collimators are on movable stages for alignment.

3.1. The neutral beamline and the suppression of the halo neutrons

The J-PARC accelerator is the most powerful proton accelerator in its energy range. For the slow extracted beam, which KOTO uses, 300 kiloWatt of 30 GeV proton beam is expected to be delivered. This intensity is about 100 times higher than the KEK-PS proton source.

A schematic drawing of the beamline²¹ is shown in Fig. 3. About 20 million K_L^0 's per beam spill (0.7 second over the 3.3 second cycle)²² are expected at the exit of the beamline by scaling the 2010 beam survey result measured with a lower beam intensity. The measured K_L^0 flux of 20 million/spill is about twice the expectation in the proposal.²⁰

Beamline collimators are designed to suppress the halo neutron. And the beam survey in 2010 confirmed the beam profile shown in Fig. 4. The ratio of the halo neutrons to the beam core neutron is roughly improved by better than an order of magnitude compared to E391a.²¹

Improving a factor of ten from E391a is hardly enough to reach the Standard Model sensitivity of the $K_L^0 \rightarrow \pi^0 \nu \bar{\nu}$ decay. The bigger suppression of halo neutron background comes from rearranging two detectors surrounding the beam. They are the Neutron Collar Count (NCC, or CC02 in E391a) and the Charged Veto (CV).

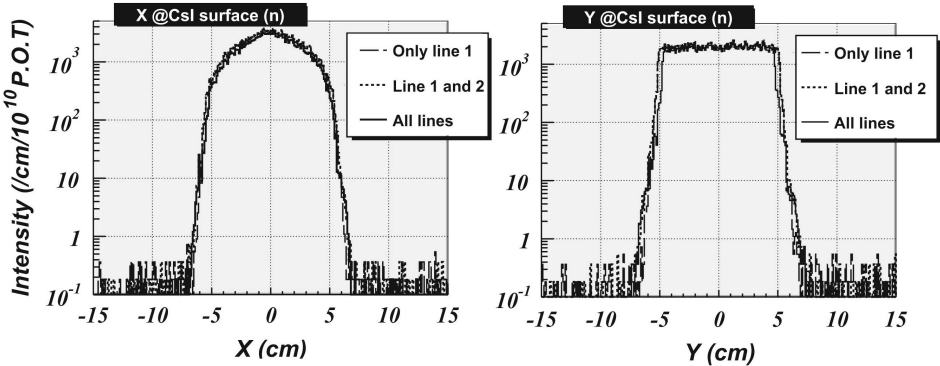


Fig. 4. The beam profile at the CsI calorimeter. P.O.T. stands for protons on target. The difference of the beam core shape in the vertical (Y) and horizontal (X) directions was due to the target image difference in the two directions.

The sampling calorimeter CC02 is replaced with NCC made of fully active material — CsI. And it is moved further away from the decay region.

For CV, a single layer of plastic scintillators was employed in E391a. To cover the whole calorimeter, part of the CV was extended 50 cm along the beam and was scraping the beam. There are two layers of CV in KOTO as shown in Fig. 2. The front layer is further away from the beam to reduce the number of interactions. The rear layer covers the entire calorimeter and sits right next to the calorimeter. The neutron interactions in the rear CV result in single clusters in the calorimeter only, and would not fake the two photons in the signal. The section scraping the beam in E391a is eliminated KOTO.

In addition to the geometry change, halo neutron interaction is further suppressed by the thinner CV — 3 mm in KOTO versus 6 mm in E391a. The charged veto inefficiency is not sacrificed by using thinner plastic plates. This is achieved by having higher quantum efficiency Multi-Pixel Photon Counters and better light collection. Preliminary result from the test run in June 2012 showed an overall inefficiency of $< 10^{-3}$, which is sufficient for the purpose.

3.2. The main calorimeter

The KOTO calorimeter consists of 2716 blocks of 50 cm long CsI crystals. The 27 radiation length calorimeter practically contains all electromagnetic (EM) showers in the KOTO energy range. This is important because photons passing through the E391a 30 cm long CsI calorimeter without interacting (punch-through) was a major cause for $K_L^0 \rightarrow \pi^0 \pi^0$ background contribution.¹⁹ Figure 5²⁰ shows the great reduction in the photon punch-through probability. Together with the detection efficiency improvements in the main barrel, the $K_L^0 \rightarrow \pi^0 \pi^0$ background is largely suppressed.²⁰

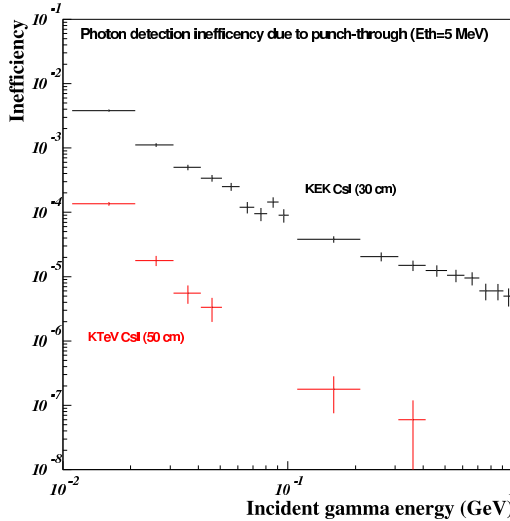


Fig. 5. Simulated photon punch-through effect in CsI.

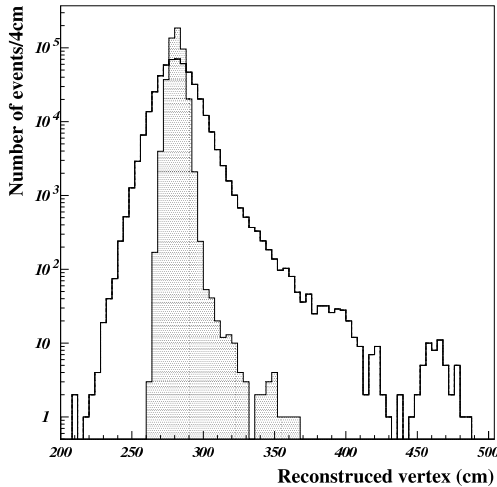


Fig. 6. Shower leakage and energy resolution of the calorimeters (simulation). Left: ratio of deposited energy over the incident photon energy. Right: reconstructed π^0 vertex, where π^0 's are produced at the E391a CC02 position in simulation.

The energy resolution is much better than the E391a calorimeter as the EM shower leaking behind the calorimeter is mostly gone. Better energy resolution is powerful in reducing the NCC-related halo neutron background as shown in Fig. 6.²⁰

The 2716 KOTO crystals covers the same area that the 576 E391a crystals covered. The finer segmented calorimeter measures photon position better and resolves photons spatially close to each other (fusion).

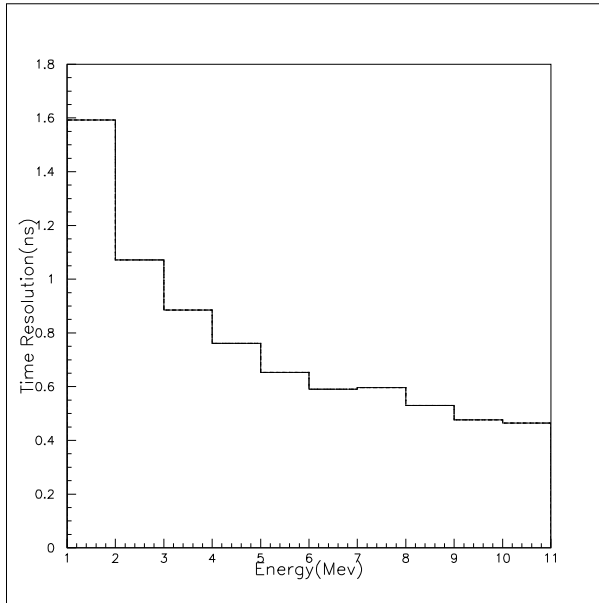


Fig. 7. Time resolution as a function of energy. The time resolution is better for higher energy photons as the pulse become smoother with more photoelectrons.

3.3. The front-end electronics

To record the details of each detector pulse in the photon detection, all KOTO detector channels except the ones in the beam are read out by 125 MHz waveform digitization boards based on flash ADCs. With the high intensity beam at J-PARC, the single rate at individual detector channel could be as high as few MHz. A typical CsI calorimeter pulse is about 100 nanoseconds wide. The 125 MHz waveform digitization is necessary to resolve pile-ups.

One unique feature of the ADC board is that it measures the time as well as the energy. To do so, a 10-pole filter is designed to shape the pulses into a quasi-Gaussian pulse before sampling. The fitted shape effectively increases the timing information compared with the standard threshold TDC technique. The simulation result of the time resolution with the fitted pulse technique is shown in Fig. 7.²³

The data output of the ADC chips is stored in a pipeline memory in a FPGA chip on the same board to avoid dead time in data taking. Fiber readout from the ADC makes the high data throughput possible. A two-leveled trigger and data acquisition system transfers data to a PC farm.

3.4. The beam hole photon veto

The beam hole photon veto detector is about 6 meters downstream from the calorimeter. While there are photons from the dominant $K_L^0 \rightarrow \pi^0 \pi^0$ background traveling in the beam core, the n/K_L^0 ratio is expected to around 20. The beam

hole photon detector is an aerogel Cerenkov counter to be insensitive to neutron interactions, and to detect the Cerenkov light produced by the photon converted electrons and positrons with high efficiency.²⁰ A 500 MHz flash ADC waveform digitizer without pulse filtering is built to cope with the harsh condition in the beam.

4. Future Prospects

The KOTO experiment is expected to complete the detector in the fall of 2012. The primary proton beam power is expected to be a few tens of kiloWatt at the beginning. With a few month of data taking the KOTO experiment will start to constrain various models beyond the Standard Model. We expect the Standard Model sensitivity could to be reached with few years of data taking pending accelerator performance and detector performance.

Acknowledgments

This work is supported in part by the US Department of Energy.

References

1. M. Kobayashi and K. Maskawa, *Prog. Theor. Phys.* **49** (1973) 652.
2. J. H. Christenson *et al.*, *Phys. Rev. Lett.* **13** (1964) 138.
3. KTeV Collab. (A. Alavi-Harati *et al.*), *Phys. Rev. Lett.* **83** (1999) 22.
4. CERN NA48 Collab. (A. J. Bevan *et al.*), *Phys. Lett. B* **465** (1999) 335.
5. BaBar Collab. (B. Aubert *et al.*), *Phys. Rev. Lett.* **89** (2002) 201802.
6. Belle Collab. (K. Abe *et al.*), *Phys. Rev. D* **66** (2002) 071102.
7. LHCb Collab. (R. Aaij *et al.*), *Phys. Rev. Lett.* **108** (2012) 111602.
8. S. Barr *et al.*, *Phys. Rev. D* **20** (1979) 2494.
9. A. Buras *et al.*, *Rev. Mod. Phys.* **80** (2008) 965.
10. J. Brod *et al.*, *Phys. Rev. D* **83** (2011) 034030.
11. M. Gaillard *et al.*, *Phys. Rev. D* **10** (1974) 897.
12. J. Ellis *et al.*, *Nucl. Phys. B* **10** (1976) 213.
13. L. Littenberg, *Phys. Rev. D* **39** (1989) 3322.
14. G. Belanger, *Phys. Rev. D* **43** (1991) 140.
15. G. Graham *et al.*, *Phys. Lett. B* **295** (1992) 169.
16. M. Weaver *et al.*, *Phys. Rev. Lett.* **72** (1994) 3758.
17. A. Alavi-Harati *et al.*, *Phys. Rev. D* **61** (2000) 072006.
18. J. Adams *et al.*, *Phys. Lett. B* **447** (1999) 240.
19. J. K. Ahn *et al.*, *Phys. Rev. D* **81** (2010) 072004.
20. J-PARC E14 Collab. (J. Comfort *et al.*), *Proposal for $K_L^0 \rightarrow \pi^0 \nu \bar{\nu}$ Experiment at J-PARC* (2006), http://osksn2.hep.sci.osaka-u.ac.jp/~taku/jparcKL/jparc_E14-proposal.pdf.
21. T. Shimogawa *et al.*, *Nucl. Instrum. Methods Res. A* **623** (2010) 585.
22. K. Shiomi *et al.*, *Nucl. Instrum. Meth. Res. A* **664** (2012) 264.
23. J. Ma *et al.*, *The Bessel Filter Simulation*, Internal Technical Notes (2007), http://hep.uchicago.edu/cpv/bessel_filter.pdf.